Hydrogenation Mechanisms in (Boratacycle)tantalum Analogues of Dimethylzirconocene

Caroline K. Sperry,[†] Guillermo C. Bazan,*[,†,§] and W. Donald Cotter*[,‡]

Contribution from the Department of Chemistry, University of Rochester, Rochester, New York 14627-0216, and Department of Chemistry, Mount Holyoke College, South Hadley, Massachusetts 01075

Received August 6, 1998

Abstract: The hydrogenation of Cp*[C_4H_4B-N(*i*-Pr)$_2$]TaMe_2 (**1**) (Cp* = C_5Me_5) in the presence of PMe_3 affords Cp*[C_4H_4B-N(*i*-Pr)$_2$]Ta$(H)_2(PMe_3)$ (**2**) in essentially quantitative yield. Similarly, the hydrogenation of Cp*[C_4H_4B-Me]TaMe_2 (**3**) in the presence of PMe_3 affords Cp*[C_4H_4B-Me]Ta$(H)_2(PMe_3)$ (**4**). Hydrogenation of **1** and **3** is accompanied by the reversible formation of side products. The most important of these complexes, Cp*[C_4H_4B-N(*i*-Pr)$_2$]Ta$(PMe_3)_2$ (**5**) and Cp*[C_4H_4B-Me]Ta$(PMe_3)_2$ (**6**), react slowly with dihydrogen forming **2** and **4**, respectively. In the early stages of the hydrogenation of **1**, the C−H activation product Cp*[C_4H_4B-N(*i*-Pr)$_2$]Ta$(H)(CH_2PMe_2)$ (**7**) is also present. Mechanistic details of the hydrogenation of **1** and **3** are discussed. Hydrogenation of [C_5H_5B-Ph][C_4H_4B-N(*i*-Pr)$_2$]TaMe_2 (**8**) in the presence of PMe_3 affords [C_5H_5B-Ph][C_4H_4B-N(*i*-Pr)$_2$]Ta$(PMe_3)_2$ (**9**) as the exclusive product. The use of a bulkier phosphine, P(*i*-Pr)$_3$, gives [C_5H_5B-Ph]-[C_4H_4B-N(*i*-Pr)$_2$]Ta$(H)_2$[P(*i*-Pr)$_3$] (**10**). Changing the phosphine to one of intermediate bulk, PEt_3, leads to the formation of *trans*-[C_5H_5B-Ph][C_4H_4B-N(*i*-Pr)$_2$]Ta$(H)_2(PEt_3)$ (**11t**). The cis isomer (**11c**) is observable during early reaction times. **11c** is a classical dihydride, perturbed by an unsymmetric three-center/two-electron interaction with the boron of the boratabenzene ligand. Isomerization of **11c** to **11t** proceeds via phosphine loss followed by kinetically detectable rearrangement of the unsaturated intermediate prior to phosphine recoordination. Treatment of **11c** with excess PMe_3 results in the formation of **9** via a mixed-phosphine intermediate, [C_5H_5B-Ph][C_4H_4B-N(*i*-Pr)$_2$]Ta$(PEt_3)(PMe_3)$ (**12**). The addition of $[H(OEt_2)_2][B(C_6H_3(CF_3)_2]$ to **11c** results in the protonation of the nitrogen atom of the borollide ligand (**H-11c**$^+$). **H-11c**$^+$ is stable at room temperature for over a week. Treatment of **10** with excess PMe_3 affords [C_5H_5B-Ph][C_4H_4B-N(*i*-Pr)$_2$]Ta$(H)_2$-(PMe_3) (**13**). Upon thermolysis in the presence of a large excess of PMe_3, **13** is converted to **9**. A mechanistic scheme for the hydrogenation of complexes such as **1** is proposed.

Introduction

The hydrogenation of group 4 metallocene dialkyls to their corresponding dihydride complexes has been studied in some detail.[1] Interest in this type of reaction stems from the importance of metal-mediated dihydrogen activation in many stoichiometric and catalytic processes.[2] Understanding the elementary molecular processes involved in this class of reactions should ultimately lead to more efficient catalysts and improved industrial processes. The most commonly accepted mechanism for the reaction of Cp_2ZrMe_2 (Cp = C_5H_5) with H_2 involves direct cleavage[1d] via a four-center/four-electron transition state (also known as σ-bond metathesis).[3] Early proposals for this mechanism discussed the importance of a weak direct interaction between the H_2 σ-bond and the zirconium-based LUMO. On the basis of the different hydrogenation rates of complexes of type $Cp_2ZrR(X)$, Schwartz suggested that the Lewis acidic Zr(IV) center polarizes the coordinated H−H bond.[1e] Hückel-type calculations led Brintzinger to invoke back-donation from the Zr−C bond into the σ^* orbital of the precoordinated H_2 molecule.[1f]

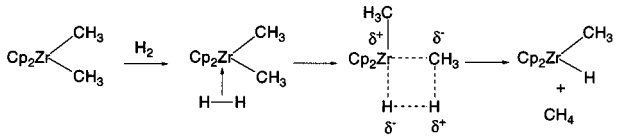

Alternative, low-energy pathways for hydrogenolysis appear to be available. In particular an oxidative addition/reductive

† University of Rochester.

‡ Mount Holyoke College.

§ Current address: Department of Chemistry, University of California, Santa Barbara, CA 93106.

(1) (a) Jordan, R. F.; Bajgur, C. S.; Dasher, W. E.; Rheingold, A. L. *Organometallics* **1987**, *6*, 1041−1051. (b) Couturier, S.; Gautheron, B. *J. Organomet. Chem.* **1978**, *157*, C61−C63. (c) Wolczanski, P. T.; Bercaw, J. E. *Organometallics* **1982**, *1*, 793−799. (d) Halpern, J. *J. Phys. Chem.* **1959**, *63*, 398−403. (e) Gell, K. I.; Posin, B.; Schwartz, J.; Williams, G. M. *J. Am. Chem. Soc.* **1982**, *104*, 1846−1855. (f) Brintzinger, H. H. *J. Organomet. Chem.* **1979**, *171*, 337−344. (g) McAlister, D. R.; Erwin, D. K.; Bercaw, J. E. *J. Am. Chem. Soc.* **1978**, *100*, 5966−5968. (h) Lee, H.; Desrosiers, P. J.; Guzei, I.; Rheingold, A. L.; Parkin, G. *J. Am. Chem. Soc.* **1998**, *120*, 3255−3256.

(2) (a) Parshall, G. W.; Ittel, S. D. *Homogeneous Catalysis;* Wiley: New York, 1992; pp 25−50. (b) James, B. R. *Homogeneous Hydrogenation*; Wiley: New York, 1973. (c) James, B. R. Hydrogenation Reactions Catalyzed by Tansition Metal Complexes. *Adv. Catal.* **1979**, *17*, 319. (d) James, B. R. In *Comprehensive Organometallic Chemistry*; Abel, E. W., Stone, F. G. A., Wilkinson, G., Eds.; Pergamon Press: New York, 1982; Vol. 8. (e) McQuillen, F. J. *Homogeneous Hydrogenation in Organic Chemisty*; D. Reidel: Dordrecht, 1976. (f) Chaloner, P. A. *Handbook of Coordination Catalysis in Organic Chemistry*; Butterworth: London, 1986. (g) Rylander, P. *Catalytic Hydrogenation in Organic Sytnheses*; Academic Press: New York, 1979. (h) Rylander, P. *Hydrogenation Methods*; Academic Press: New York, 1985. (i) Chaloner, P. A.; Esteruelas, M. A.; Joó, F.; Oro, L. A. *Homogeneous Hydrogenation*; Kluwer Academic Publishers: Dordrecht, 1994.

10.1021/ja982803g CCC: $18.00
Published on Web 02/09/1999

elimination sequence is of interest. Such a pathway formally requires the participation of six electrons, two of which must originally reside on the metal.[4] Given that zirconium in Cp_2ZrMe_2 is in its highest oxidation state, it is difficult to consider this mechanism directly without prior cyclopentadienyl ligand rearrangement. Bercaw has suggested that the Cp* (Cp* = C_5Me_5) ligand can participate directly in an intramolecular rearrangement, which generates a formally reduced (Zr(II)) metal center.[1g] Oxidative addition followed by reductive elimination leads to rapid ($t_{1/2} \approx 5$ min at −15 °C, 1 atm of H_2) formation of products. This mechanism accounts for the distribution of products derived from isotopomers of $Cp^*_2ZrH(CH_2CHMe_2)$ and H_2.

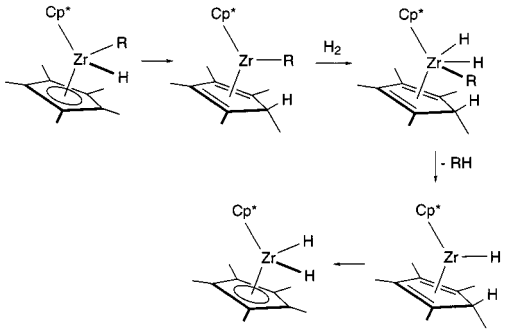

Different mechanistic variants have thus been proposed for the hydrogenation of ziroconocene complexes, and the choice of ancillary ligand appears to influence the preferred pathway.

In general, such reactions are slow under moderate (*ca*. 1 atm) pressures of dihydrogen. Jordan has estimated $t_{1/2}$ for the hydrogenolysis (1 atm of H_2) of Cp_2ZrMe_2 in THF at >86 h.[1a] Synthetic procedures for preparation of zirconocene dihydrides via hydrogenolysis of dimethyl precursors typically call for elevated (60−100 atm) pressures of H_2.[1b] The most facile reported hydrogenation of a simple dimethylzirconocene derivative, $Cp^*_2ZrMe_2$, can be conducted under 1 atm of H_2, but requires an extended reaction time (1 week) and somewhat elevated temperatures (70 °C).[5]

We recently reported a preliminary study on the hydrogenolysis of Cp*[C_4H_4B-N(*i*-Pr)$_2$]TaMe_2 (**1**, see Table 1), which contains the dianionic borollide ligand, [C_4H_4B-N(*i*-Pr)$_2$]$^{2-}$.[6] Complex **1** is isostructural and may be considered in some respects (e.g., formal electron count at the metal) isoelectronic to group 4 metallocene dialkyls. However, the rate of reaction with dihydrogen of **1** is about 3 orders of magnitude faster than that of Cp_2ZrMe_2 and at least 2 orders of magnitude faster than that of $Cp^*_2ZrMe_2$.[7] This faster rate allows us to probe the hydrogenation process more readily and to detect short-lived intermediates which may not be apparent in the slower processes.

Table 1. Compound Abreviation Index

compd no.	compd formula
1	Cp*[C_4H_4B-N(*i*-Pr)$_2$]TaMe_2
2	Cp*[C_4H_4B-N(*i*-Pr)$_2$]Ta$(H)_2(PMe_3)$
3	Cp*[C_4H_4B-Me]TaMe_2
4	Cp*[C_4H_4B-Me]Ta$(H)_2(PMe_3)$
5	Cp*[C_4H_4B-N(*i*-Pr)$_2$]Ta$(PMe_3)_2$
6	Cp*[C_4H_4B-Me]Ta$(PMe_3)_2$
7	Cp*[C_4H_4B-N(*i*-Pr)$_2$]Ta$(H)(CH_2PMe_2)$
8	[C_5H_5B-Ph][C_4H_4B-N(*i*-Pr)$_2$]TaMe_2
9	[C_5H_5B-Ph][C_4H_4B-N(*i*-Pr)$_2$]Ta$(PMe_3)_2$
10	[C_5H_5B-Ph][C_4H_4B-N(*i*-Pr)$_2$]Ta$(H)_2$[P(*i*-Pr)$_3$]
11c/t	[C_5H_5B-Ph][C_4H_4B-N(*i*-Pr)$_2$]Ta$(H)_2(PEt_3)$
12	[C_5H_5B-Ph][C_4H_4B-N(*i*-Pr)$_2$]Ta$(PEt_3)(PMe_3)$
13	[C_5H_5B-Ph][C_4H_4B-N(*i*-Pr)$_2$]Ta$(H)_2(PMe_3)$

In this contribution, we present a more detailed mechanistic account of the hydrogenation of **1** and related molecules. We argue that the relative rates of activation of H_2 by **1** and related complexes are understood by a reaction energy profile (σ-bond metathesis reaction) dominated by the stability of the dihydrogen adduct as originally suggested by Brintzinger.[1f] We show evidence that the final hydride product is a result of H_2 oxidative addition to a low-valent intermediate produced by reductive elimination of CH_4 from Cp*[C_4H_4B-N(*i*-Pr)$_2$]Ta(H)Me. Finally, from an analysis of the hydrogenation profile of related compounds, we delineate the pathway by which oxidative addition of H_2 produces the dihydride products.

Results and Discussion

Hydrogenation of 1. As shown in eq 1, the addition of H_2 to **1** in the presence of PMe_3 affords Cp*[C_4H_4B-N(*i*-Pr)$_2$]Ta$(H)_2(PMe_3)$ (**2**) in essentially quantitative yield, as determined by NMR spectroscopy. When Cp*[C_4H_4B-Me]TaMe_2 (**3**) is used, the final product is Cp*[C_4H_4B-Me]Ta$(H)_2(PMe_3)$ (**4**). Phosphine is required in these reactions to stabilize the dihydride products.

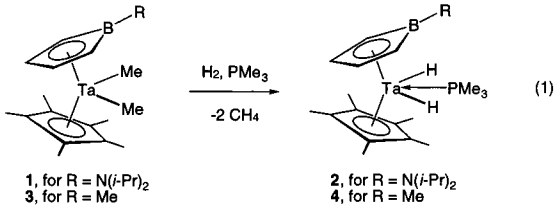

The rates of disappearance of both **1** and **3** are linearly dependent on the concentration of starting material and dihydrogen pressure, at least in the limited range of pressures accessible for NMR spectroscopy studies (Figure 1). Under identical reaction conditions **1** is consumed more rapidly than **3** by a factor of approximately 3.8 (Figure 2).

The electronic structures of **1** and **3** are affected by the nature of the exocyclic substituent on boron.[8] Complexes containing

(3) (a) Thompson, M. E.; Bercaw, J. E. *Pure Appl. Chem.* **1984**, *56*, 1−11. (b) Steigerwald, M. L.; Goddard, W. A., III *J. Am. Chem. Soc.* **1984**, *106*, 308−311. (c) Thompson, M. E.; Baxter, S. M.; Bulls, A. R.; Burger, B. J.; Nolan, M. C.; Santarsiero, B. D.; Schaefer, W. P.; Bercaw, J. E. *J. Am. Chem. Soc.* **1987**, *109*, 203-219. (d) Rappé, A. K. *Organometallics* **1990**, *9*, 466−475. (e) Ziegler, T.; Folga, E.; Berces, A. *J. Am. Chem. Soc.* **1993**, *115*, 5, 636−646.

(4) (a) Crabtree, R. H. *The Organometallic Chemistry of the Transition Metals*, 2nd ed.; Wiley: New York, 1994. (b) Lukehart, C. M. *Fundamental Transition Metal Organometallic Chemistry*; Brooks-Cole: Pacific Grove, 1985. (c) Yamamoto, A. *Organotransition Metal Chemistry*; Wiley-Interscience: New York, 1986. (d) Collman, J. P.; Hegedus, L. S.; Norton, J. R.; Finke, R. G. *Principles and Applications of Organotransition Metal Chemistry*; University Science Books: Mill Valley, 1987.

(5) Schock, L. E.; Marks, T. J. *J. Am. Chem. Soc.* **1988**, *110*, 7701−7715.

(6) Kowal, C. M.; Bazan, G. C. *J. Am. Chem. Soc.* **1996**, *118*, 10317−10318.

(7) Detailed kinetic studies have not been performed, and qualitative published reports conflict concerning the rate of hydrogenolysis of $Cp^*_2ZrMe_2$. Sanner (Miller, F. D.; Sanner, R. D. *Organometallics* **1988**, *7*, 818−825) reports that this reaction requires one week at ca. 100 atm of H_2. We base our comparison on Marks' report (one week to completion at 70 °C, cited above) and a reaction time of about an hour for complete consumption of **1**; the temperature difference is not accounted for here. Jordan has cautioned that comparisons of Cp−Zr and Cp*−Zr fragments in this context are complicated by the fact that Cp* may induce alternative mechanisms.[1a]

(8) Herberich, G. E.; Hessner, B.; Ohst, H.; Raap, I. A. *J. Organomet. Chem.* **1988**, *348*, 305−316.

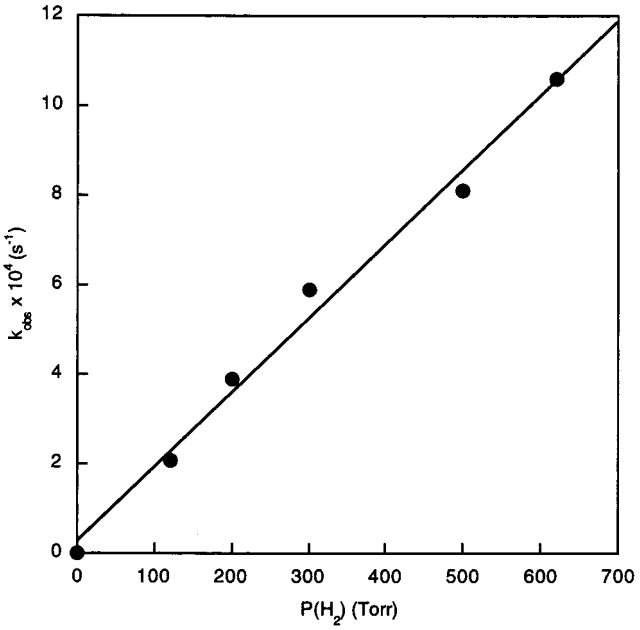

Figure 1. Observed rates for the disappearance of **1** ($[Ta]_o = 0.038$ M) in C_6D_6 with 5 equiv of PMe_3.

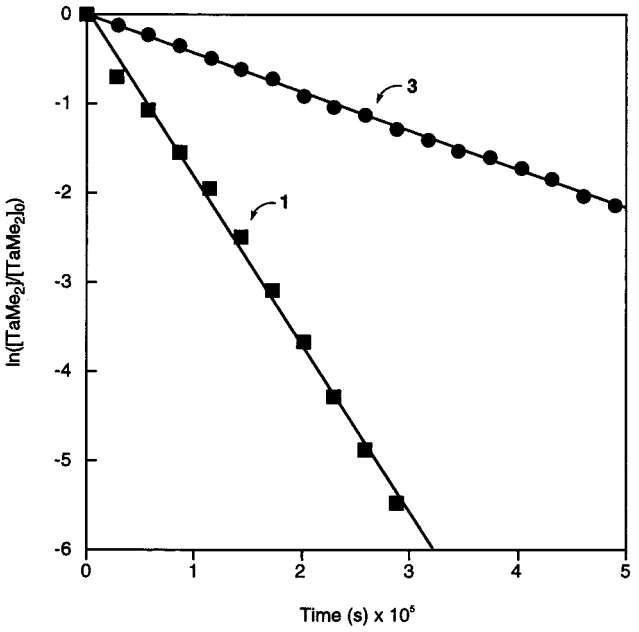

Figure 2. Representative data for the disappearance of **1** and **3** in C_6D_6 ($[Ta]_o = 0.022$ M, $P(H_2) = 620$ Torr, 5 equiv of PMe_3).

the aminoborollide ligand are formally ambivalent since three resonance structures are required to describe the metrical parameters of their crystallographically determined structures.

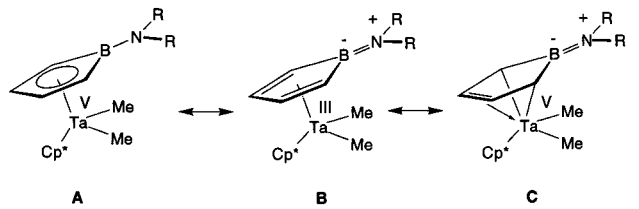

The boron atom in the methylborollide ligand cannot form a π bond with the exocyclic group and thus **3** is best described by the high-valent structure corresponding to resonance contribution **A**, as shown above.[9]

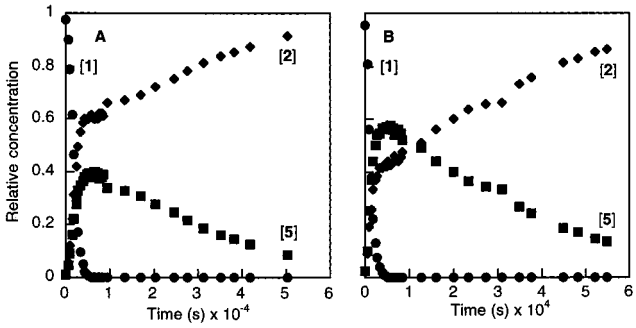

Figure 3. Concentration profile of **1**, **2**, and **5** as a function of $[PMe_3]$: (A) 5 equiv of PMe_3; (B) 9 equiv of PMe_3.

Scheme 1

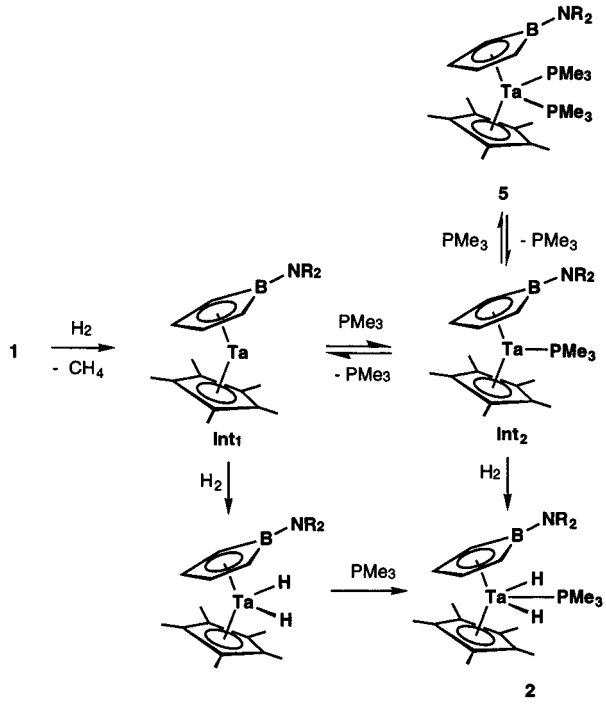

Increasing the concentration of phosphine does not affect the rate of consumption of **1** or **3** but decreases the rate of appearance of **2** or **4**, producing instead larger amounts of a new organometallic species, namely Cp*[C_4H_4B-N(*i*-Pr)$_2$]Ta-(PMe_3)$_2$ (**5**) or Cp*[C_4H_4B-Me]Ta(PMe_3)$_2$ (**6**). Figure 3 shows the concentration profiles of **1**, **2**, and **5** for different PMe_3 concentrations. As the concentration of PMe_3 increases the ratio of **2** to **5** at early reaction times shifts in favor of **5**. Figure 3 also shows that the concentration of **2** increases sharply while **1** is present in solution, after which a second, slower process takes place. The two distinct slopes for the appearance of product require two independent paths for its production. In our initial contribution we proposed that, in the case of **1**, the common intermediate for the two paths is Cp*[C_4H_4B-N(*i*-Pr)$_2$]Ta.[6] Oxidative addition of H_2 followed by trapping with PMe_3 forms **2**. Alternatively, Cp*[C_4H_4B-N(*i*-Pr)$_2$]Ta coordinates 2 equiv of PMe_3 to give **5**. Loss of phosphine, followed by H_2 addition represents the slower process for formation of **2**. Scheme 1 summarizes our original proposed mechanism.

Careful determination of mass balance in the ^{1}H NMR spectra of the reaction mixtures reveals the presence of an additional species. As shown in Figure 4, this species is observed at

(9) Sperry, C. K.; Cotter, W. D.; Lee, R. A.; Lachicotte, R. J.; Bazan, G. C. *J. Am. Chem. Soc.* **1998**, *120*, 7791−7805.

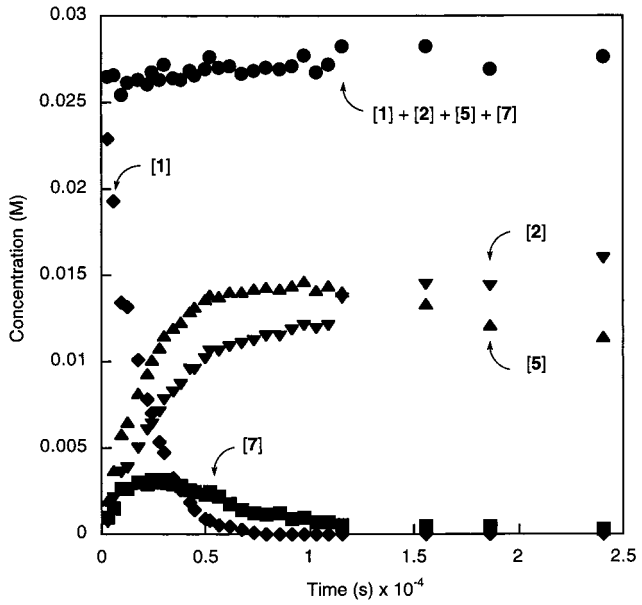

Figure 4. Full concentration profile for the disappearance of **1**, with mass balance.

Scheme 2

$$\mathbf{5} \underset{}{\overset{K_1}{\rightleftharpoons}} \mathbf{Int_2} + PMe_3 \xrightarrow{k_2[H_2]} \mathbf{2}$$

$$\frac{d[2]}{dt} = \frac{K_1 k_2 [H_2][5]}{[PMe_3]}$$

$$(k_{obs})^{-1} = \frac{[PMe_3]}{k_1 k_2 [H_2]}$$

significant concentrations during and immediately after consumption of **1**. It is characterized by the appearance of an additional Cp* resonance (15 H) and a pair of high-field doublets (1 H each). These doublets are coupled to a resonance in the ^{31}P NMR spectrum of the reaction mixture at δ −50.3 (J_{PH} = 5.0 Hz). The spectral features of this species are consistent with a phosphinomethanide structure, Cp*[C_4H_4B-N(*i*-Pr)$_2$]Ta(H)-(CH_2PMe_2) (**7**), with an uncoordinated phosphorus atom.[10] We have not been able to locate the hydride resonance for **7**. However, its structural assignment is supported by the observation that when PMe_3-d_9 is used in place of PMe_3, the appearance of the characteristic doublets is completely suppressed, demonstrating that they originate from the phosphine methyl groups. The rate of disappearance of **1** is not affected by the isotopic constitution of PMe_3, but the rate of formation of **7** is much slower in the presence of PMe_3-d_9 ($k_H/k_D \approx 3-4$), indicating substantial perturbation of the C−H bond in PMe_3 in the rate-determining step for the formation of **7**.

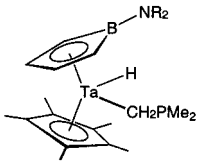

7

(10) In isoelectronic zirconocene systems, $Cp_2Zr(Cl)CH_2PR_2$, the ^{31}P chemical shift for the η^1 isomer resembles closely that of the free phosphine while the chemical shift of the η^2 isomer is similar to that of the coordinated phosphine. (a) Karsch, H. H.; Denbelly, B.; Hoffmann, J.; Pieper, U.; Müller, G. *J. Am. Chem. Soc.* **1988**, *11*, 3654−3656. (b) Karsch, H. H.; Müller, G.; Krüger, C. *J. Organomet. Chem.* **1984**, *273*, 195−212.

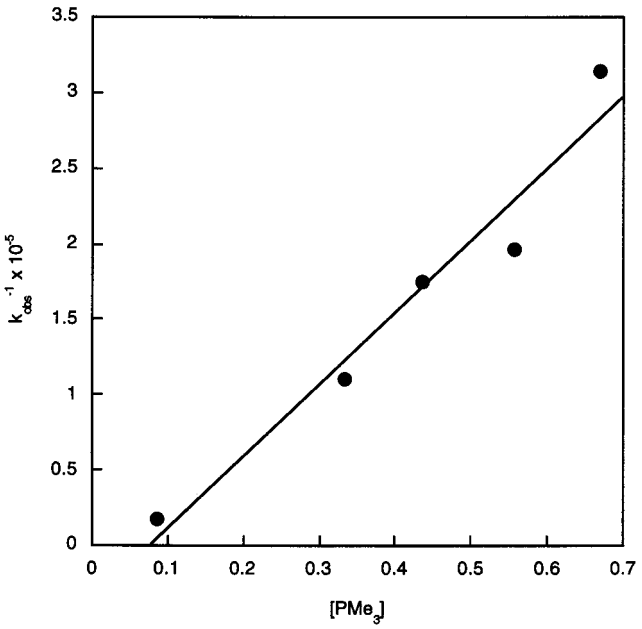

Figure 5. Phosphine dependence for conversion of **5** to **2**.

In an attempt to define better the relative importance of the reactive hydrogenation intermediate (i.e., **Int$_1$** or **Int$_2$** in Scheme 1), the kinetics of hydrogenation for compound **5**, generated in situ from hydrogenation of **1**, were studied (eq 2). The rate of disappearance of **5** was measured by ^{1}H NMR spectroscopy at 25 °C, after complete consumption of **1**. In the presence of varying concentrations of PMe_3 (ca. 0.1−0.6 M, $[Ta]_0$ = 0.023 M), the rate of loss of **5** was identical to the formation rate of **2** and obeyed pseudo-first-order kinetics in PMe_3 over at least 3 half-lives.

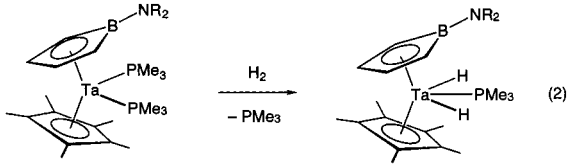

5 **2** (2)

The results of the late-reaction kinetic studies are shown in Figure 5. Hydrogenation of **5** is suppressed by PMe_3, as anticipated. A plot of $(k_{obs})^{-1}$ vs $[PMe_3]$ is linear in the concentration range used in these studies[11] and passes through an intercept of approximately zero.[12] These observations are accounted for by a mechanism in which compound **5** participates in a rapid (relative to subsequent addition of H_2) equilibrium with a small amount of **Int$_2$** (Scheme 2). The first-order suppression of the rate by $[PMe_3]$ indicates that loss of both phosphine ligands to form the "naked" tantalum species **Int$_1$** does not occur to a detectable extent. The formation of **Int$_1$** in kinetically significant amounts during the early stages of hydrogenolysis, i.e., before complete consumption of **1**, is not necessarily contradicted by these observations.

(11) It is not immediately obvious that pseudo-first-order kinetics should apply in the case of relatively small excesses of phosphine, e.g., 5 equiv, but they do. In this case, at the point of complete consumption of **1** about 75% of the total Ta is present as the final product, **2**. PMe_3 is thus present in approximately a 14-fold excess compared to the reactive species, **5**. In all cases, $[PMe_3]$ is corrected for the amount of phosphine retained by **5** and **2** at full consumption of **1**.

(12) The apparent negative intercept $(-4(3) \times 10^4)$ is not significant compared to the uncertainty in the measurement.

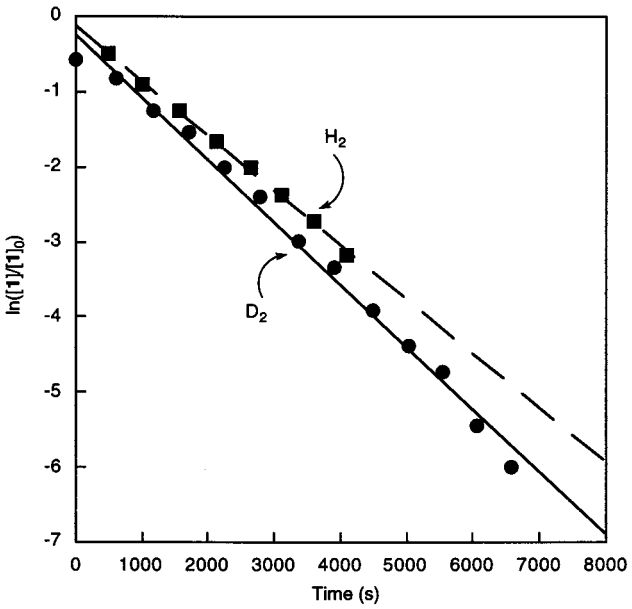

Figure 6. First-order rate plots for the reaction of **1** with H_2 and D_2 ($k_H = 7.2(1) \times 10^{-4}$ s^{-1}; $k_D = 8.3(2) \times 10^{-4}$ s^{-1}; $k_H/k_D = 0.87(9)$).

Scheme 3

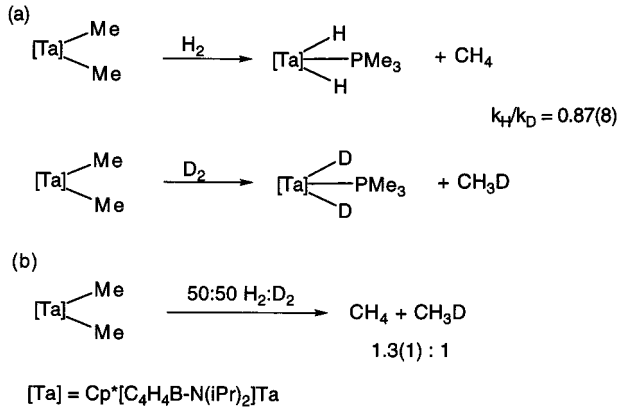

The hydrogenation of **1** in the absence of phosphine provides an intermediate that ultimately leads to a yet unidentified product.[6] Spectroscopic characterization for the intermediate is consistent with the formula Cp*[C_4H_4B-N(*i*-Pr)$_2$]TaH_2. In one experiment the intermediate concentration was maximized and the solution was immediately subjected to 3 freeze−pump−thaw cycles to remove as much solvated hydrogen as possible. At that stage an excess of PMe_3 was condensed into the reaction mixture and allowed to react. ^{1}H NMR spectroscopy showed that only **2** had formed. No **5** could be detected. These experiments strongly suggest that the intermediate we observe is Cp*[C_4H_4B-N(*i*-Pr)$_2$]TaH_2 and that this compound is inert to reductive elimination of H_2. Formation of **5** would have implicated a facile reductive elimination step.

A set of kinetic deuterium isotope effect measurements were made to probe the nature of dihydrogen activation by **1** (Scheme 3). When the rate of disappearance of **1** (in benzene) is measured independently with H_2 and D_2 (Scheme 3a), the ratio k_{H_2}/k_{D_2} is approximately 0.87(9) (Figure 6). The magnitude of this ratio and the error associated with its determination indicate no kinetic isotope effect within statistical certainty. In a separate experiment, equal pressures of H_2 and D_2 were thoroughly mixed in a high-vacuum manifold and added to a benzene solution containing **1** and 5 equiv of PMe_3 (Scheme 3b). ^{1}H NMR

Scheme 4

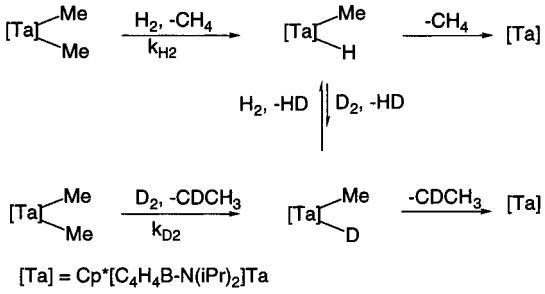

Scheme 5

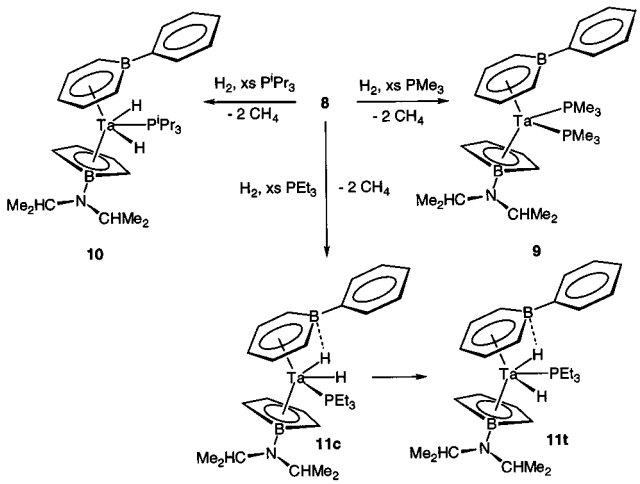

analysis of the methane produced revealed an isotopomer ratio of 1.3(1):1 (CH_4:CH_3D).[13]

The discrepancy between the kinetic isotope effect for consumption of starting material and the isotopomer distribution in the products from the 50:50 H_2/D_2 reaction indicates the presence of an intermediate capable of H/D exchange. We propose that the intermediate is Cp*[C_4H_4B-N(*i*-Pr)$_2$]TaMeH (Scheme 4) and point out that [$Cp_2ZrMe(\mu\text{-}H)]_2$ forms in the reactions of Cp_2ZrMe_2 with low pressures of H_2.[1a] Consistent with this proposal, a fleetingly observable species appears, in very low concentrations, in the early stages of hydrogenation of **1**, identified by a methyl resonance at δ −0.64 ppm. This resonance is a doublet in reaction mixtures containing H_2 ($^3J_{HH}$ = 4.4 Hz), but a singlet under D_2, indicating coupling to a single proton derived from gaseous dihydrogen. We cannot identify this species more accurately, but these spectroscopic properties are consistent with a methyl hydride structure. We tentatively assign it as Cp*[C_4H_4B-N(*i*-Pr)$_2$]TaMeH. The higher ratio of CH_4 relative to CH_3D in the presence of an excess mixture of H_2 and D_2 indicates an equilibrium isotope effect on the scrambling process, in which Ta−H is preferred relative to Ta−D.

Hydrogenation of [C_5H_5B-Ph][C_4H_4B-N(*i*-Pr)$_2$]TaMe_2 (8). The relationship between boratabenzene and cyclopentadienyl ligands has been studied in some detail.[14] Since both ligands are 6 π electron donors it is possible in many instances to exchange a Cp framework within a complex for a boratabenzene

(13) The solubilities of H_2 and D_2 in benzene are very similar. The solubility of D_2 exceeds that of H_2 by 3%. Cook, M. W.; Hanson, D. N.; Alder, B. J. *J. Chem. Phys.* **1957**, *26*, 748−751.

(14) For a recent review of boratabenzene complexes see: Herberich, G. E. In *Comprehensive Organometallic Chemistry II*; Abel, E. W., Stone, F. G. A., Wilkinson, G., Eds.; Pergamon Press: Oxford, 1995; Vol. 1, p 197.

counterpart without gross changes in molecular geometry or electronic structure. Recent advances in the area of metallocene-like complexes supported by boratabenzene have shown that the selectivity of important catalytic reactions can be controlled by the exocyclic boron substitutent.[15] It occurred to us that replacement of Cp* in **1** with a boratabenzene ligand would result in complexes which react with H_2 in a similar fashion but which could lead to the detection of intermediates not observable in the hydrogenation of **1**. In this section we describe the hydrogenation chemistry of $[C_5H_5B\text{-}Ph][C_4H_4B\text{-}N(i\text{-}Pr)_2]TaMe_2$ (**8**), including the characterization of important intermediates and processes undetectable with Cp* complexes.

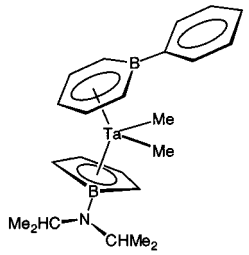

8

When **8** is treated with H_2 in the presence of PMe_3 the only product obtained is $[C_5H_5B\text{-}Ph][C_4H_4B\text{-}N(i\text{-}Pr)_2]Ta(PMe_3)_2$ (**9** in Scheme 5). No intermediates are observed by ^1H NMR spectroscopy. Formation of a dihydride complex fails, even at H_2 pressures of 15−20 atm.[16] Changing the phosphine to bulkier $P(i\text{-}Pr)_3$ allows for the quantitative formation of $[C_5H_5B\text{-}Ph][C_4H_4B\text{-}N(i\text{-}Pr)_2]Ta(H)_2(P(i\text{-}Pr)_3)$ (**10** in Scheme 5), analogous to **2**.

Use of a phosphine of intermediate bulk, PEt_3, leads eventually to formation of *trans*-$[C_5H_5B\text{-}Ph][C_4H_4B\text{-}N(i\text{-}Pr)_2]Ta(H)_2(PEt_3)$ (**11t** in Scheme 5). The crystallographically determined molecular structure of **11t** has been shown to be largely similar to those of **2** and **4**, except that it shows evidence of a Ta−H−B three-center interaction with the boratabenzene boron atom.[17]

Monitoring the progress of the reaction with PEt_3 reveals a different dihydride species during early reaction times. Variable-temperature ^1H and $^{31}P\{^1H\}$ NMR spectra show that this intermediate is the *cis*-dihydride (**11c** in Scheme 5) that rearranges to form the thermodynamically preferred **11t**. The room-temperature spectrum of **11c** in THF-d_8 contains one doublet for the rapidly exchanging pair of hydrides ($\delta = -2.80$; $J_{PH} = 48$ Hz). The borollide and boratabenzene protons are diastereotopic. At low temperature ($T = 198$ K), two inequivalent hydride signals are observed. The different values of J_{PH} for the two inequivalent hydrides allow for the assignment of the endo and exo hydride signals ($\delta_{endo} = -2.60$, $J_{PH} = 86.5$ Hz; $\delta_{exo} = -3.19$, $J_{PH} = 9.2$ Hz).[18]

Complex **11c** is isoelectronic with a series of tantalum dihydride complexes studied by Chaudret.[18] Both classical and nonclassical dihydride ground states have been established, depending on the supporting ligands on Ta. In general, electron-withdrawing ligands favor dihydrogen adduct formation by reducing the magnitude of back-bonding into σ^*_{HH}. Thus, *cis*-$[Cp_2Ta(H_2)CO]^+$ is a dihydrogen adduct in the ground state, while cis-$\{Cp_2Ta(H)_2[P(OMe)_3]\}^+$ is a classical dihydride. Complex **11c** adopts a classical structure, as shown by the absence of detectable HD coupling in the NMR spectrum of **11c-*d*$_1$**.[19] Chaudret has shown that the H−H distance (r_{HH}) in *cis*-tantalocene dihydrides can be estimated reliably from spin−lattice relaxation data, using the T_1(min) value for the trans isomer to correct for interactions other than hydride−hydride relaxation. The T_1 value for **11c** passes through a minimum of 165 ms at 248 K;[20] for **11t**, T_1(min) = 358 ms at 208 K. With use of the approximation that motion about the H−H vector is slow compared to τ_c (245 ps at 400 MHz), the equations described by Morris[21] yield $r_{HH} = 1.76$ Å for **11c**. The H−H distance in **11c** is comparable to that determined for the classical dihydride cis-$\{Cp_2Ta(H)_2[P(OMe)_3]\}^+$ (1.67 Å),[18] and to the H−H separation observed in the neutron diffraction structure of Cp_2TaH_3 (1.85 Å), and it is thoroughly consistent with a classical dihydride ground state. The low-valent resonance structure **B** presumably renders the tantalum atom in **11c** sufficiently electron-rich to favor the dihydride despite the inductive effect anticipated from the two boron atoms in the cyclic ligands.

Further structural information about **11c** is found in the ^{11}B NMR spectra. The boron atom in coordinated borollide and boratabenzene normally resonates near 30 ppm (relative to $BF_3{\cdot}OEt_2$) in electrophilic complexes. For example, the boratabenzene and borollide borons in **8** resonate at 36.5 and 34.9 ppm, respectively. Exceptions occur when boron participates in a three-center interaction with a hydride ligand, as has been reported previously for **11t**.[9] The boratabenzene boron is significantly shifted in **11t**, to 19 ppm, and a three-center interaction with one of the hydride ligands was confirmed by X-ray analysis. The ^{11}B NMR signal for the boratabenzene boron in **11c** is similarly shifted, resonating at 10.8 ppm, compared to 30.8 ppm for the borollide boron. Thus, a three-center interaction is also indicated in **11c**, most probably with the exo hydride. The Ta−H−B interaction for **11c** appears to be stronger than that in **11t**, as the boron signal is even further upfield.

11c is thus a classical dihydride complex, perturbed by an unsymmetric three-center/two-electron interaction with boron. However, the balance between classical and nonclassical structures is clearly a delicate one in tantalum sandwich compounds.[19] The possibility of a low-lying dihydrogen tautomer cannot be dismissed. The chemical behavior of **11c** is consistent with this possibility. In particular, the hydride ligands are very labile. H/D exchange of the hydrides in **11c** is complete within 5 min under 1 atm of D_2.

Displacement of the two hydride ligands by trimethylphosphine is also rapid. Thus, treatment of **11c** with excess PMe_3 in the presence of dihydrogen gas results in loss of H_2 and formation of **9**. $^{31}P\{^1H\}$ and ^1H NMR spectroscopies reveal the

(15) (a) Rogers, J. S.; Bazan, G. C.; Sperry, C. K. *J. Am. Chem. Soc.* **1997**, *119*, 9305−9306. (b) Bazan, G. C.; Rodriguez, G.; Ashe, A. J., III; Al-Ahmad, S.; Müller, C. *J. Am. Chem. Soc.* **1996**, *118*, 2291−2292. (c) Bazan, G. C.; Rodriguez, G.; Ashe, A. J., III; Al-Ahmad, S.; Kampf, J. W. *Organometallics* **1997**, *16*, 2492−2494.

(16) We would like to thank Dr. Emilio Bunel for these experiments.

(17) Herberich, G. E.; Carstensen, T.; Köffer, D. P. J.; Klaff, N.; Boese, R.; Hyla-Kryspin, I.; Gleiter, R.; Stephan, M.; Meth, H.; Zenneck, U. *Organometallics* **1994**, *13*, 619−630.

(18) Sabo-Etienne, S.; Chaudret, B.; Abou el Makarim, H.; Barthelat, J.-C.; Daudey, J.-P.; Ulrich, S.; Limbach, H.-H.; Moïse, C. *J. Am. Chem. Soc.* **1995**, *117*, 11602−11603.

(19) (a) Kubas, G. J.; Ryan, R. R.; Swanson, B. I.; Vergamini, P. J.; Wasserman, H. J. *J. Am. Chem. Soc.* **1984**, *106*, 451−452. (b) Kubas, G. J. *Acc. Chem. Res.* **1988**, *21*, 120−128. (c) Rattan, G.; Kubas, G. J.; Unkefer, C. J.; Van Der Sluys, L. S.; Kubat-Martin, K. A. *J. Am. Chem. Soc.* **1990**, *112*, 3855−3860.

(20) The values for the exo and endo hydrides are, in fact, slightly different. We use the T_1(min) value for the endo hydride in this calculation, as the slightly shorter T_1(min) for the exo hydride (160 ms at 248 K) may be perturbed by contributions from the quadrupolar boron nucleus.

(21) (a) Bautista, M. T.; Earl, K. A.; Maltby, P. A.; Morris, R. H.; Schweitzer, C. T.; Sella, A. *J. Am. Chem. Soc.* **1988**, *110*, 7031−7036. (b) Earl, K. A.; Jia, G.; Maltby, P. A.; Morris, R. H. *J. Am. Chem. Soc.* **1991**, *113*, 3027−3029.

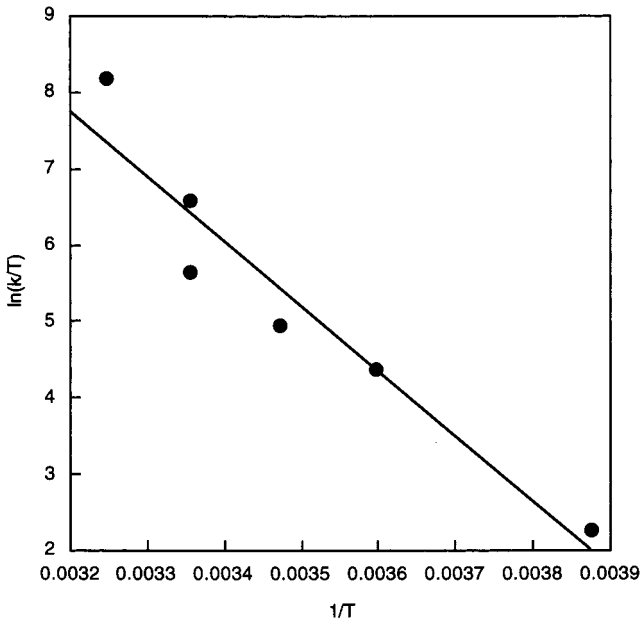

Figure 7. Eyring plot for fluxional hydride exchange in **11c**.

complete formation of an intermediate species within 3 min of PMe_3 addition. Subsequent conversion to **9** occurs over approximately 40 min at room temperature ([Ta] = 0.0228 M). The intermediate species contains both coordinated PMe_3 and PEt_3 ligands. Thus, we identify the intermediate as the mixed-phosphine complex $[C_5H_5B\text{-}Ph][C_4H_4B\text{-}N(i\text{-}Pr)_2]Ta(PEt_3)(PMe_3)$ (**12** in eq 3).

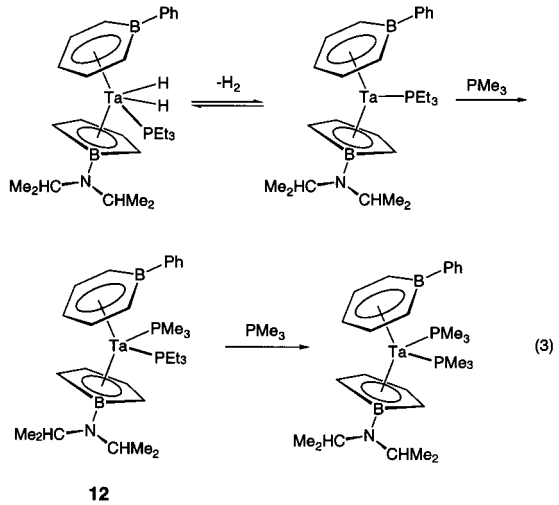

12

The dissociative nature of hydrogen loss from **11c** is shown by the independence of the rate of formation of **12** on $[PMe_3]$. The observed rate constants were found to be identical (0.02-(2) s^{-1}) in the presence of 0.114 and 0.456 M PMe_3. Although fairly rapid for standard NMR kinetics, these rates could be measured by generating a C_6D_{12} solution of **11c** in an NMR sample tube, adding PMe_3 to the frozen reaction mixture, and inserting the sample tube into a room temperature probe immediately upon thawing.

Close examination of the endo/exo hydride exchange process in **11c** also suggests the likelihood of an energetically accessible dihydrogen adduct. Above the coalescence point,[22] the $^1H\{^{31}P\}$ NMR signal from the averaged hydrides appears as a simple singlet with a temperature-dependent line width. Rate constants for exchange were extracted from these spectra by conventional line-shape analysis.[23] Eyring analysis over a 50 K range provides the activation parameters, $\Delta H^{\ddagger} = 16(2)$ kcal/mol, $\Delta S^{\ddagger} = 21(8)$ eu (Figure 7). The borollide and boratabenzene ring protons remain diastereotopic at all temperatures, indicating that the process by which the hydride ligands are interchanged does not alter the configuration at tantalum. This restriction precludes exchange via dissociation or coordination of phosphine. Exchange most likely occurs by formation of an intermediate dihydrogen adduct that rotates in place (eq 4).[24]

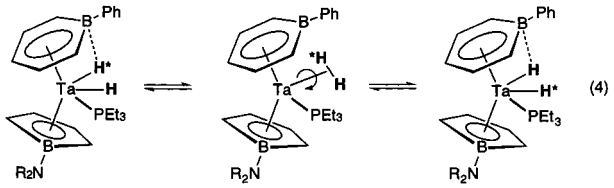

$\Delta H^{\ddagger}$ for hydride exchange in **11c** thus incorporates contributions from (i) the enthalpy required to convert the classical to the nonclassical structure, (ii) disruption of the exo hydride/boron interaction, and (iii) in situ rotation of coordinated H_2. Rotation of coordinated H_2 in a tantalocene-like wedge is accompanied by a $\Delta H^{\ddagger}$ of about 10 kcal/mol (estimated from $\Delta H^{\ddagger}$ for the nonclassical dihydride *cis*-$Cp_2Ta(H_2)(CO)^+$, 9.6 kcal/mol), placing an upper bound on contributions i and ii of about 6 kcal/mol.[19] Interestingly, $\Delta H^{\ddagger}$ for intramolecular exo/endo exchange in **11c** is essentially identical with the value measured for cis-$\{Cp_2Ta(H)_2[P(OMe)_3]\}^+$ (16.6 kcal/mol), a classical dihydride in which the stabilizing boron−hydride interaction is not possible.[18]

Isomerization of 11c to 11t. The kinetics of hydrogenation of **8** show a phosphine dependence unlike that observed for hydrogenation of **1**. Increasing the concentration of PEt_3 does not alter the rate of formation of **11c**, nor does it result in the formation of a bis-phosphine adduct. Rather, a weak but detectable suppression of the rate of isomerization from **11c** to **11t** is observed (Figure 8). This is an unexpected observation, because the most obvious mechanisms for isomerization give rise to rate laws which are independent of phosphine concentration. An exclusively intramolecular mechanism, e.g., one in which rearrangement occurs via hydride migration to the boron atom of the boratabenzene ring, is immediately excluded by the observation of phosphine inhibition. A simple dissociative mechanism in which loss of phosphine is followed by rate-determining trapping of a symmetrical, intermediate dihydride to form **11t** (Scheme 6a) is also excluded. Phosphine suppression of the rate can be best accommodated by a kinetically significant step after phosphine dissociation that does not itself involve phosphine. As shown in Scheme 6b, an appropriate rate law results from a mechanism in which the initial dihydride intermediate (**Int$_4$**) retains its cis configuration, with the empty site occupying an exo position. Subsequent rearrangement to a *trans*-like geometry, in which the exo positions are occupied

(22) At temperatures near and below the coalescence point, the spectra display complex line shapes, particularly when phosphorus coupling is retained. The unusual appearance of these spectra may be due to interactions with quadrupolar ^{11}B.

(23) Sandstrøm, J. *Dynamic NMR Spectroscopy*; Academic Press: New York, 1982.

(24) At the present time we cannot exclude an exchange process whereby one hydride "hops" to the boratabenzene boron atom, followed by separation of H and P within the metallocene-like wedge, rotation of the boratabenzene ligand, and reattachment of the hydride at the alternate site. We currently disfavor such an exchange on two grounds: (a) such a mechanism would significantly increase the positive charge at Ta, and (b) the activation parameters for exchange are very similar to those reported by Chaudret for systems in which boron is absent.

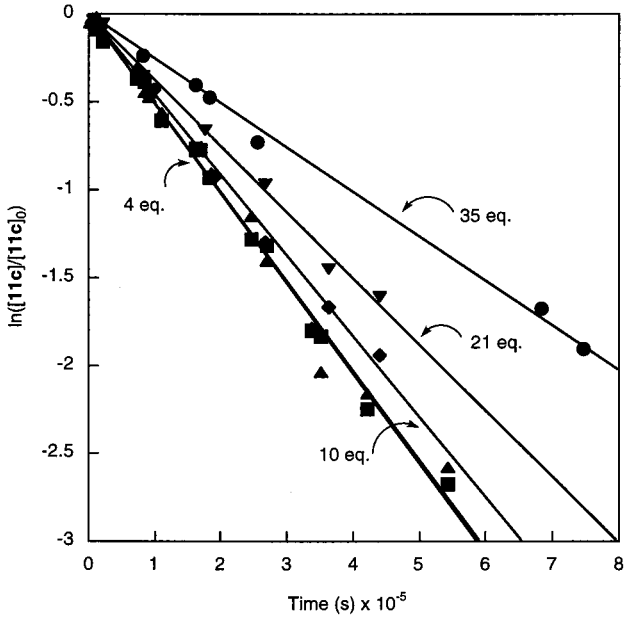

Figure 8. Rates of isomerization of **11c** to **11t** in C_6D_{12} ($[Ta]_o = 0.023$ M; $[PEt_3] = 0.096$, 0.144, 0.240, 0.480, 0.800 M; $P(H_2) = 620$ Torr).

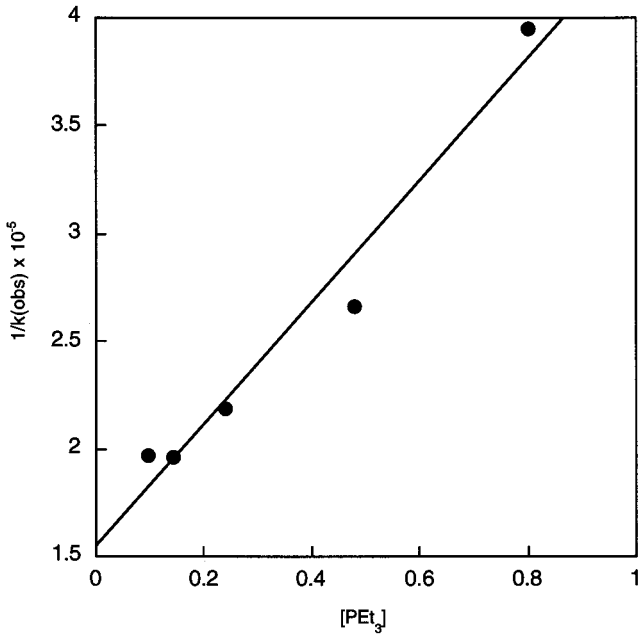

Figure 9. $(k_{obs})^{-1}$ vs $[PEt_3]$ for isomerization of **11c** to **11t**.

Scheme 6

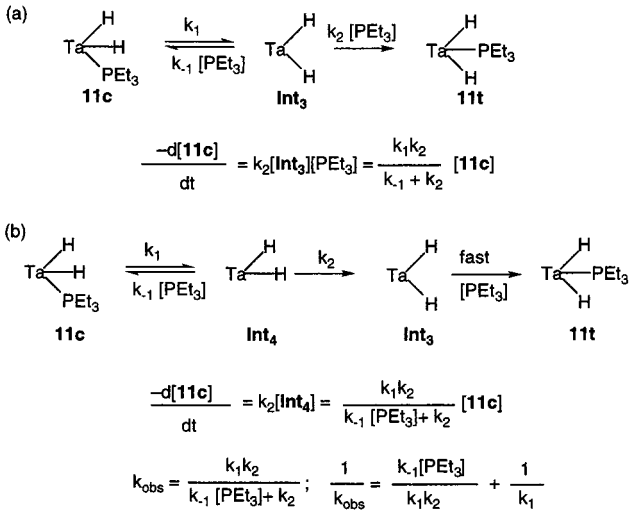

by hydride ligands and the empty site lies in the endo position, constitutes an intramolecular "trapping" step. A plot of $(k_{obs})^{-1}$ vs $[PEt_3]$ is linear, as shown in Figure 9. The intercept yields the rate constant for phosphine loss from **11c** ($k_1 = 6.5 \times 10^{-6}$ s^{-1}). Rearrangement and phosphine trapping are closely competitive in rate ($k_{-1}/k_2 = 1.8$); both are presumably quite fast.

Finally, the stablity of the cis dihydride is sensitive to the nature of exocyclic substitution on the borollide ligand. Thus, treatment of **11c** with $[H(OEt_2)_2][B(C_6H_3(CF_3)_2]$[25] results in protonation of the nitrogen atom in the borollide ligand (**H-11c**$^+$). As has been shown for other borollide complexes, such protonation eliminates the contribution of the low-valent Ta resonance structure **B**.[26] **H-11c**$^+$ is stable in THF-d_8 at room temperature for over a week. We attribute this stability to a slower rate of phosphine dissociation as a result of the increased Ta−P bond strength in the more electron deficient **H-11c**$^+$.

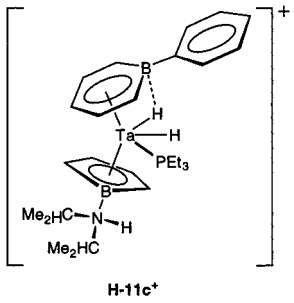

Synthesis and Thermodynamic Instability of $[C_5H_5B\text{-}Ph][C_4H_4B\text{-}N(i\text{-}Pr)_2]Ta(H)_2(PMe_3)$ (13). Hydrogenation of the dimethyl complexes **1** and **3** produces both high-valent (i.e. hydrides **2** and **4**) and low-valent (phosphine complexes **5** and **6**) products, but in both cases the high-valent hydrides are the final, stable products. The sole formation of the bis-phosphine adduct **9**, when **8** is hydrogenated in the presence of PMe_3, to the exclusion of any hydride products, is thus remarkable. To determine whether this preference for **9** arises from thermodynamic or kinetic factors, we sought to make the corresponding hydride complex by an alternative route.

Treatment of $[C_5H_5B\text{-}Ph][C_4H_4B\text{-}N(i\text{-}Pr)_2]Ta(H)_2[P(i\text{-}Pr)_3]$ (**10**) with excess PMe_3 rapidly affords $[C_5H_5B\text{-}Ph][C_4H_4B\text{-}N(i\text{-}Pr)_2]Ta(H)_2(PMe_3)$ (**13**) as the exclusive product, identified by its ^1H and $^{31}P\{^1H\}$ NMR spectra (eq 5).

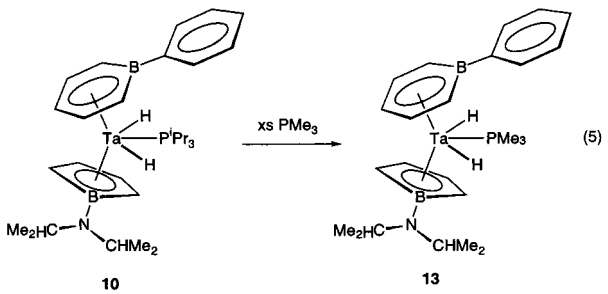

(5)

Most diagnostic of **13** is the doublet at −2.64 ppm (2 H, $J_{PH} = 64.3$ Hz), corresponding to the two hydride ligands. Upon thermolysis at 65 °C for one month, in the presence of 1 atm

(25) Brookhart, M.; Grant, B.; Volpe, A. F., Jr. *Organometallics* **1992**, *11*, 3920−3921.

(26) (a) Herberich, G. E.; Englert, U.; Hostalek, M.; Laven, R. *Chem. Ber.* **1991**, *124*, 17−23. (b) Ashe, A. J., III; Kampf, J. W.; Müller, C.; Schneider, M. *Organometallics* **1996**, *15*, 387−393. (c) Bazan, G. C.; Donelly, S. J.; Rodriguez, G. *J. Am. Chem. Soc.* **1995**, *117*, 2671−2672.

Scheme 7

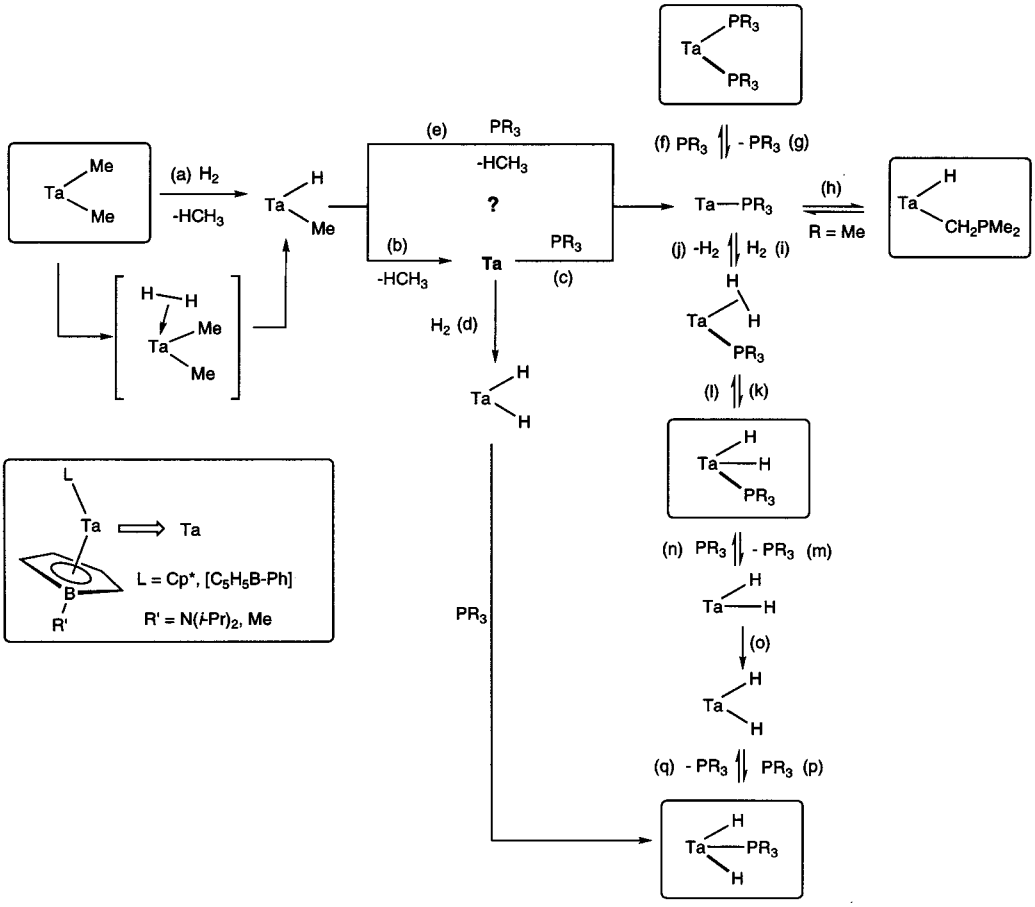

of H_2 and 10 equiv of PMe_3 ([PMe_3] = 0.37 M), **13** is converted to the bis-phosphine complex **9**.[27] **9** is thus the thermodynamically stable product under these conditions and the activation barrier separating the two species is rather high. That the dihydride is favored for every other case in this study suggests to us that the two structures are thermodynamically quite close in energy. The Ta centers in **9** and **13** are particularly electron deficient (vis-à-vis **2** and **5**) due to the substitution of electron-rich Cp* with the electron-deficient phenylboratabenzene. This increased electrophilicity, coupled with the smaller size of PMe_3 relative to PEt_3 and $P(i\text{-}Pr)_3$, apparently creates a particularly strong Ta−P bond in **9**.

Summary and Conclusion

Despite their potential utility, little is systematically known on how boratacyclic analogues of cyclopentadienyl perturb the reactivity of classical organometallic fragments. The results of this contribution show that the hydrogenation mechanisms of complexes **1**, **3**, and **8** are considerably different than those observed previously with the isoelectronic group 4 metallocenes and reveal new aspects of the elementary reaction chemistry of dihydrogen. Scheme 7 presents a series of steps that brings together many of the observations described in this paper. This reaction sequence can be usefully broken down into four stages: (i) initial activation of dihydrogen by high-valent tantalum, release of methane, and generation of a reactive, low-valent tantalum fragment (**Ta** in Scheme 7, Steps a and b), (ii) partitioning of **Ta** among two reaction pathways (Steps c and d), (iii) partitioning of a monophosphine adduct among three reaction pathways (Steps f, h, and i), and (iv) approach and activation of dihydrogen by a low-valent tantalum site (Steps d or i−q).

The evidence reported here does not allow for a definitive account of the initial activation of dihydrogen by **1**, **3**, and **8** (Step a). We have argued elsewhere, on the basis of a comparison of crystal structure data for a large series of tantalum−borollide complexes, that the ground state of compound **1** is strongly influenced by the low-valent resonance structure **B**.[9] Bercaw and co-workers also noted that the electronic spectra of related aminoborollide−zirconium and −hafnium complexes support the view of an ambivalent, and correspondingly electron rich, ground state.[28] As such, the formally d^2 tantalum raises the possibility that oxidative addition of H_2 is allowed. We currently do not favor such a mechanism because the consumption of starting material is not significantly different between **1** and **3**. Unlike the aminoborollide complexes, **3** is best defined as strictly Ta(V), and thus is not subject to further formal oxidation.

At the present time, Brintzinger's "direct hydrogen transfer" mode provides the most consistent rationale for the relative rates of the four-center/four-electron activation of H_2 by **1**, **3**, and their slower zirnonocene analogues.[1f] The essential features are (i) precoordination of H_2 to the metallocene-like fragment and (ii) a transition state in which both H atoms and the carbon atom maintain substantial overlap with the metal. Although the

(27) One atmosphere of dihydrogen was introduced to the NMR tube after excess PMe_3 was added. The tube was shaken vigorously at regular intervals while being heated.

(28) (a) Kiely, A. F.; Nelson, C. M.; Pastor, A.; Henling, L. M.; Day, M. W.; Bercaw, J. E. *Organometallics* **1998**, *17*, 1324−1332. (b) Pastor, A.; Kiely, A. F.; Henling, L. M.; Day, M. W.; Bercaw, J. E. *J. Organomet. Chem.* **1997**, *528*, 65−75.

net result is the formal transfer of H^+ to CH_3^-, the migrating hydrogen does not build a substantial partial positive charge along the reaction pathway. In the direct hydrogen transfer reaction, the reactivity of the weakly coordinated H_2 ligand controls the rate of hydrogenation.[29] The decrease in reactivity toward H_2 with increasing electron deficiency (**1** > **3** ≫ Cp_2ZrMe_2) is simply accounted for by the electronic demand anticipated for direct hydrogen transfer. Increasing electron density at the metal center weakens the H−H interaction by promoting back-bonding into the σ^*_{HH}.

The evolution of the second equivalent of methane most likely takes place by reductive elimination from an intermediate methyl hydride species, producing the highly reactive, low-valent tantalum intermediate **Ta** (Step b). Similar reactivity is observed with Cp_2WHMe, which reductively eliminates CH_4 and provides $[Cp_2W]$.[30] If one considers the low-valent resonance structure **B** for **1** then both **1** and Cp_2WHMe can be described as isoelectronic species with d^2 metal centers. With the information available at this time it is not possible to rule out a phosphine-induced reductive elimination as shown by Step e. However, our observations of the hydrogenation of **1** in the absence of phosphine show that an associative process is not required for the clean formation of a reactive dihydride (TaH_2). Intramolecular elimination of CH_4 from the methyl hydride therefore seems to us the simplest proposal. If a bare intermediate (**Ta**) forms, its lifetime in solution is exceedingly short. Once trapped by phosphine it is not likely to be regenerated (i.e., by ligand loss) in kinetically significant concentrations.

Three choices are available to the monophosphine adduct. Addition of another equivalent of PMe_3 (Step f) forms bisphosphine species such as **5**, **6**, or **9**. Intramolecular C−H activation affords a phosphinomethanide hydride such as **7** (Step h). The third option is reaction with H_2 (Step i).

We have been able to observe the interaction between dihydrogen and the low-valent fragment derived from **8** in remarkable detail. Steps i through q in Scheme 7 constitute a composite of several observations that, when taken together, delineate the approach and activation of H_2 and subsequent rearrangement of the organometallic species to the final product. As dihydrogen approaches it chooses a site next to phosphorus within the metallocene wedge and the formation of a σ-adduct ensues. Back-bonding from tantalum weakens the H−H interaction giving a classical dihydride (Step k). Supporting these initial steps are the exchange of hydrides in **11c** and the facile displacement of H_2 from **11c**, as well as the work by Chaudret that has shown the small differences in energies between dihydrogen adducts and dihydrides in the isoelectronic Cp_2Ta^+ core.[18] Isomerization from a *cis*-dihydride to a trans configuration (Step o) takes place after phosphine decoordination (Step m). Our studies of the isomerization of **11c** to **11t** suggest that rearrangement of the phosphine-free, *cis*-dihydride species is competitive with coordination of phosphine (Step n). While most of these elementary steps have literature precedent it is difficult to obtain a metal−ligand system for which such an overarching hydrogenation sequence can be constructed. The ability to detect evidence for hydrogen motion within the metallocene wedge is unique and is probably a result of the three-center/two-electron interaction between Ta, B, and H. No such restraint exists in standard metallocenes, and the sliding of the two hydrides is expected to require less energy. It is probably effortless.

In summary, substitution of boratacyclic ligands for cyclopentadienyls within an isoelectronic metallocene framework reveals new metal-mediated elementary reactions. It is not inherent that the hydrogenation mechanism be the same for families of compounds represented by **1** and Cp_2ZrMe_2. Rather, the study of the $[C_4H_4B\text{-}N(i\text{-}Pr)_2]Ta$ framework increases our awareness of alternative mechanistic pathways that may be operative in compounds containing the Cp_2Zr core. From a broader perspective, the boratacycle for Cp substitution represents a useful strategy to probe the mechanisms of previously inaccessible reactions.

Experimental Section

General Considerations. All manipulations were carried out with either high-vacuum or glovebox techniques as previously described.[31] ^1H, ^{31}P, ^{11}B, and ^{13}C NMR spectra were recorded on a Bruker AMX-400 spectrometer at 400.1, 161.97, 128.3, and 100.6 MHz, respectively. ^{11}B and ^{31}P spectra were taken with use of $BF_3{\cdot}OEt_2$ and H_3PO_4 respectively as external references. ^1H and ^{13}C were taken with use of internal references. H_2 and D_2 gases were purchased from Cambridge Isotope Labs and passed through oxygen scavengers to remove any residual water or oxygen. Toluene, benzene, pentane, diethyl ether, and tetrahydrofuran were distilled from benzophenone ketyl. PMe_3-d_9, PEt_3, and $P(i\text{-}Pr)_3$ were purchased and used as received from Aldrich. The preparations of **1**,[26c] **2**,[26c] **3**,[6] **4**,[6] **5**,[6] **6**,[6] **8**,[9] and **9**[9] are available in the literature.

General Procedure for Hydrogenation Reactions. A stock solution was prepared by dissolving **1** (60.7 mg, 0.114 mmol) and ferrocene (10.6 mg, 0.0570 mmol) in C_6D_{12} (2500 μL). Samples were prepared by adding this stock (250 μL) and the desired quantity of PMe_3 to an NMR tube equipped with a Teflon needle valve, followed by enough C_6D_{12} to bring the total volume to 500 μL. The sample was then degassed via 3 freeze−pump−thaw cycles, and H_2 was added over the frozen liquid. Liquid nitrogen coolant was applied only to the level of solution in the tube. The sample was thawed for at least 1 min prior to insertion into an NMR probe (298 K). During the kinetic runs, the sample was removed from the probe and shaken vigorously for 10 s at regular intervals during the disappearance of starting material to ensure efficient mixing of gaseous H_2 into the solution. After starting material was completely consumed, the sample was then placed on a rotation device at room temperature and returned periodically to the NMR probe for observation.

Preparation of $[C_5H_5B\text{-}Ph][C_4H_4B\text{-}N(i\text{-}Pr)_2]Ta(H)_2(P(i\text{-}Pr)_3)$ (10). To a solution of $[C_5H_5B\text{-}Ph][C_4H_4B\text{-}N(i\text{-}Pr)_2]TaMe_2$ (25 mg, 0.047 mmol) in toluene-d_8 was added $P(i\text{-}Pr)_3$ (18 μL, 0.095 mmol) via microliter syringe. The sample was degassed with use of 3 freeze−pump−thaw cycles and 563 Torr of H_2 was placed over the frozen sample. The solution was thawed and rotated for 3 days. ^1H NMR (toluene-d_8): δ 8.00 (d, 2H, *o*-C_6H_5), 7.45 (m, 2H, *m*-C_6H_5), 7.34 (t, 1H, *p*-C_6H_5), 6.24 (m, 2H, CHC*H*CHB), 5.07 (m, 2H, C*H*CHB), 5.05 (t, 1H, C*H*CHCHB), 4.27 (d, 2H, CHCHC*H*B), 3.34 (sept, 2H, CH*Me*$_2$), 2.60 (m, 2H, CHC*H*B), 1.60 (m, 3H, P(C*H*Me$_2$)$_3$), 1.24 (d, 12H, CH*Me*$_2$), 0.8 (m, 18H, P(CH*Me*$_2$)$_3$), −1.9 (d, 2H, Ta−H, J_{P-H} = 55.8 Hz). $^{13}C\{^1H\}$ NMR (toluene-d_8): δ 137.2 (C_6H_5), 134.2 (C_6H_5), 125.7 (C_6H_5), 121.7 (C_6H_5), 120.7 (CH*C*HCHB), 96.1 (b, CH*C*HB), 89.7 (*C*HCHCHB), 77.3 (*C*HCHB), 58.7 (b, CHCH*C*HB), 47.0 (*C*HMe$_2$), 25.6 (P(*C*HMe$_2$)$_3$), 24.3 (CH*Me*$_2$), 19.3 P(CH*Me*$_2$)$_3$). ^{11}B NMR (external reference $BF_3{\cdot}OEt_2$): δ 28.5 (η^5-C_4H_4B-N(*i*-Pr)$_2$), 14.7 (C_5H_5B-Ph). $^{31}P\{^1H\}$ NMR (toluene-d_8): δ 35.15 (Ta(*P*(CHMe$_2$)$_3$)).

Preparation of *cis*-$[C_5H_5B\text{-}Ph][C_4H_4B\text{-}N(i\text{-}Pr)_2]Ta(H)_2(PEt_3)$ (11c). To a solution of $[C_5H_5B\text{-}Ph][C_4H_4B\text{-}N(i\text{-}Pr)_2]TaMe_2$ (17 mg, 0.0372 mmol) in C_6D_6 was added 2 equiv of PEt_3 (10.99 μL, 0.744 mmol) via microliter syringe. The sample was degassed with use of 3 freeze−pump−thaw cycles and 434 Torr of H_2 was placed over the frozen sample. The solution was thawed and allowed to rotate for 1 h. Isolation of this complex proved unsuccessful as the isomerization to **11t** occurs even at −35 °C. ^1H NMR (C_6D_6): δ 8.16 (d, 2H, *o*-C_6H_5), 7.47 (m,

(29) Density functional calculations point to the dihydrogen adduct as the lowest energy species in the hydrogenation of Cp_2ScMe. See ref 3e.

(30) (a) Bullock, R. M.; Headford, C. E. L.; Hennessy, K. M.; Kegley, S. E.; Norton, J. E. *J. Am. Chem. Soc.* **1989**, *111*, 3897−3908. (b) Green, M. L. H. *Pure Appl. Chem.* **1984**, *56*, 47.

(31) Burger, B. J.; Bercaw, J. E. In *Experimental Organometallic Chemistry*; Wayda, A. L., Darensbourg, M. Y., Eds.; ACS Symp. Ser. 357; American Chemical Society, Washington, DC, 1987.

2H, *m*-C_6H_5), 7.31 (t, 1H, *p*-C_6H_5), 6.40 (m, 1H, CHC*H*CHB), 5.36 (m, 1H, C*H*CHB), 4.78 (m, 3H, CHC*H*CHB, C*H*CHCHB, C*H*CHB), 4.32 (d, 1H, CHCHC*H*B), 4.07 (d, 1H, CHCHC*H*B), 3.26 (b, 2H, C*H*Me_2), 2.93 (m, 1H, CHC*H*B), 2.48 (m, 1H, CHC*H*B), 1.03 (d, 12H, CH*Me*$_2$), 1.66 (m, 6H, TaPC*H*$_2$CH$_3$), 0.57 (m, 9H, TaPCH$_2$C*H*$_3$), −2.52 (d, 2H, TaH_2). ^{11}B NMR (external reference BF_3·OEt_2): δ 30.8 (η^5-C_4H_4*B*-N(*i*-Pr)$_2$), 10.8 (C_5H_5*B*-Ph). ^{31}P{^{1}H} NMR (THF-d_8): δ 18.7 (Ta(*P*Et_3)).

Preparation of *cis*-[C_5H_5B-Ph][C_4H_4B-N(*i*-Pr)$_2$]Ta(H)(D)(PEt_3) (11c-d_1). To prepare HD gas, NaH (2.00 g, 0.167 mol) was suspended in 30 mL of toluene. D_2O (1.67 mL, 0.835 mmol) was added via syringe under an argon purge at −78 °C. HD gas was collected in the vacuum manifold and the HD gas was placed over a degassed tube of **8** (4.93 mg, 0.00935 mmol) and Cp_2Fe (0.9 mg, 0.005 mmol) in 500 μL of C_6D_{12}. The solution was thawed and allowed to rotate for 1 h.

Preparation of *cis*-[C_5H_5B-Ph][C_4H_4B-N(*i*-Pr)$_2$]Ta(H)$_2$(PEt_3)-[B($C_6H_3(CF_3)_2)_4$] (H-11c$^+$). One equivalent of [H(OEt_2)$_2$][B(C_6H_3-$(CF_3)_2)_4$] (45.0 mg, 0.045 mmol) in THF-d_8 was added to freshly prepared **11c** (27.8 mg, 0.045 mmol). An instantaneous color change to a lighter orange/yellow occurred. ^{1}H NMR (THF-d_8): δ 7.80 (b, 10H, *o*-C_6H_5, γ-B-C_6H_3), 7.59 (s, 4H, α-B-C_6H_3), 7.36 (m, 2H, *m*-C_6H_5), 7.32 (m, 1H, *p*-C_6H_5), 6.44 (m, 2H, CHC*H*CHB), 6.25 (d, 1H, C*H*CHCHB), 6.03 (b, 1H, N-*H*), 5.16 (m, 2H, CHCHC*H*B, C*H*CHB), 5.09 (m, 1H, CHCHC*H*B), 4.99 (m, 1H, C*H*CHB), 3.56 (m, 2H, C*H*Me_2), 3.38 (m, 8H, *Et*$_2$O), 2.93 (m, 1H, CHC*H*B), 2.55 (m, 1H, CHC*H*B), 1.80 (m, 6H, P*Et*$_3$), 1.35 (m, 9H, P*Et*$_3$), 1.23 (dd, 6H, CH*Me*$_2$), 1.11 (m, 12H, *Et*$_2$O), 0.94 (dd, 6H, CH*Me*$_2$), −2.12 (d, 1H, Ta-*H*, J_{PH}=75.7 Hz), −4.48 (d, 1H, Ta-*H*, J_{PH}=10.2 Hz). ^{11}B NMR (external reference BF_3·OEt_2): δ 24.8 (η^5-C_4H_4*B*-N(*i*-Pr)$_2$), 21.2 (C_5H_5*B*-Ph), −2.76 (*B*-C_6H_3). ^{31}P{^{1}H} NMR (THF-d_8): δ 16.1 (Ta-(*P*Et_3)).

Observation of [C_5H_5B-Ph][C_4H_4B-N(*i*-Pr)$_2$]Ta(PEt_3)(PMe_3) (12). Excess PMe_3 (15.5 μL, 0.146 mmol) was added to a tube containing **11c** (7.03 mg, 0.0114 mmol) and Cp_2Fe (1.06 mg, 0.0057 mmol) in toluene-d_8. Within 3 min, **11c** had been consumed and the solution contained **12** and **9** only. ^{1}H NMR (toluene-d_8): δ 7.91 (d, 2H, *o*-C_6H_5), 7.24 (m, 2H, *m*-C_6H_5), 7.19 (t, 1H, *p*-C_6H_5), 5.15 (m, 2H, CHC*H*CHB), 4.56 (t, 1H, C*H*CHCHB), 3.65 (d, 2H, CHCHC*H*B), 3.50 (sept, 2H, C*H*Me_2), 2.30 (b, 2H, C*H*CHB), 1.85 (b, 2H, CHC*H*B), 1.45 (m, 6H, P*Et*$_3$), 1.35 (d, 9H, P*Me*$_3$), 1.04 (dd, 12H, CH*Me*$_2$), 0.86 (m, 9H, PEt_3). ^{31}P{^{1}H} NMR (C_6D_{12}): δ −2.68 (Ta(*P*Et_3), J_{PP} = 8.14 Hz), −33.1 (broad, Ta(*P*Me_3)).

Characterization of [C_5H_5B-Ph][C_4H_4B-N(*i*-Pr)$_2$]Ta(H)$_2$(PMe_3) (13). Excess PMe_3 (15.9 μL, 0.150 mmol) was added to a tube containing **10** (9.88 mg, 0.0150 mmol) in C_6D_6. Within 5 min, **13** was the exclusive product by NMR spectroscopy. ^{1}H NMR (THF-d_8): δ 7.68 (d, 2H, *o*-C_6H_5), 7.22 (m, 2H, *m*-C_6H_5), 7.14 (t, 1H, *p*-C_6H_5), 6.30 (m, 2H, CHC*H*CHB), 5.25 (t, 1H, C*H*CHCHB), 4.91 (m, 2H, C*H*CHB), 4.25 (d, 2H, CHCHC*H*B), 3.26 (sept, 2H, C*H*Me_2), 2.29 (m, 2H, CHC*H*B), 1.32 (d, 9H, PMe_3), 1.09 (d, 12H, CH*Me*$_2$), −2.64 (d, 2H, Ta-H, J_{P-H} = 64.3 Hz). ^{13}C{^{1}H} NMR (C_6D_6): δ 133.8 (C_6H_5), 128.2 (C_6H_5), 127.6 (C_6H_5), 127.2 (C_6H_5), 120.6 (CH*C*HCHB), 96.3 (b, CH*C*HB), 87.0 (*C*HCHCHB), 77.7 (*C*HCHB), 58.6 (b, CHCH*C*HB), 46.9 (*C*HMe_2), 21.0 (CH*Me*$_2$), 16.3 (P*Me*$_3$). ^{11}B NMR (external reference BF_3·OEt_2): δ 27.6 (η^5-C_4H_4*B*-N(*i*-Pr)$_2$), 14.5 (C_5H_5*B*-Ph). ^{31}P-{^{1}H} NMR (C_6D_6): δ 19.9 (Ta(*P*Me_3).

Acknowledgment. G.C.B. is an Alfred Sloan Fellow and an Henry and Camille Dreyfus Teacher Scholar. The authors are grateful to the Department of Energy and the Petroleum Research Fund for financial support of this work.

JA982803G